

POLLUTANT EMISSIONS AND STABILITY LIMITS OF A POROUS RADIANT BURNER IN A HOT ENVIRONMENT

Rafael de Camargo Catapan, catapan@labcet.ufsc.br

Mechanical Engineering Department, Federal University of Santa Catarina, Florianópolis - SC - Brazil

Amir Antonio Martins de Oliveira, amir@emc.ufsc.br

Mechanical Engineering Department, Federal University of Santa Catarina, Florianópolis - SC - Brazil

Mário Costa, mcosta@ist.utl.pt

Mechanical Engineering Department, Instituto Superior Técnico, Technical University of Lisbon, Lisbon - Portugal

Abstract. *Industry have a need for heating equipment which complies to ever more stringent emission regulations and that also provides a way of replacing existing electrical infrared by natural gas heating. Examples include processes such as ceramic tiles sintering in tunnel kilns, drying of paper and wood and thermoforming of thermoplastic parts. In the last years, few works have focused the operation of porous radiant burners (PRB) in hot environments, typical of industrial process. In this direction, a detailed experimental study of the combustion characteristics, such as the stability limits and the pollutant emissions, of a PRB in a confined hot environment is presented. A laboratory-scale furnace with control of wall temperatures was used. The local temperature and major species concentration were measured on the PRB and on the furnace, respectively. For comparisons purposes, tests in an open environment were also made. The results show that the upper stability limit (blow-out) of PRB are approximately the same for both confined and open environment operations. However, the confined environment operation was strongly limited by the porous matrix temperature, allowing only mixtures with equivalence ratio smaller than 0,60. This higher flame temperature originated a growth of NO_x emissions. Conversely, the CO emissions decreased when the furnace wall temperatures were increased.*

Keywords: combustion in porous media, porous radiant burner, pollutant emission, industrial heating

1. INTRODUCTION

Combustion in porous media has been vastly investigated due to its well-known characteristics of good flame stability, low pollutant emission, extended lean flammability limit and high radiation efficiency (see, for example, Howell et al. (1996) for a review about this theme before 1994). Here, a short review is presented with emphasis in radiating heating.

A basic porous radiant burner (PRB) design was initially proposed and analyzed by Takeno and Sato (1979) and Kotani e Takeno (1982). There, a high conductivity solid matrix was introduced within the flame region. This solid matrix transfers heat from the post-flame region to the pre-heating flame region. Early theoretical models used a single-step global reaction mechanism and assumed either the existence of local thermal equilibrium between the gas and solid phases (Kotani et al., 1984 and Yoshizawa et al., 1988) or a thermal non equilibrium (two-equation) model (Sathe et al., 1990a and Sathe et al., 1990b). More recently, a few works have considered detailed chemical kinetic mechanisms along with either thermal equilibrium (Brenner et al., 2000) or thermal non equilibrium models (Hsu et al., 1993; Hsu e Mathews, 1993; Barra e Ellzey, 2004 and Mishra et al., 2006).

The configuration of PRB that has been more investigated is formed by two ceramic foams with different properties (Hsu et al., 1993; Khanna et al., 1994; Hsu, 1996; Ellzey e Goel, 1995; Trimis e Durst, 1996; Mital et al., 1997; Pereira, 2002; Barra et al., 2003; Barra e Ellzey, 2004; Talukdar et al., 2004 e Mishra et al., 2006). The advantage of this burner configuration is that the interface between the two ceramic foams is an efficient flame holder. Consequently, the flame stability characteristics depend on the porous matrix properties. This however, may not provide a uniform temperature field in the surface of a large porous radiating burner, considering the quality of the available ceramic foams (Pereira, 2002).

In order to allow for larger surface area burners, an alternative strategy of flame stabilization in a PRB was proposed recently (Catapan et al., 2005). It consists of the injection of the premixed reactants from a perforated plate placed upstream from the ceramics foams. Each injection point becomes the place for stabilization of a single conical flame. The higher velocities of the expanding jet developed in the vicinity of the injection hole prevents flame flashback. This mechanism of flame stabilization was experimentally analyzed in a PRB with a single injection orifice (Catapan et al., 2006). The main results show that the single flame front has a conical shape, burning in both ceramics foams with different properties and is anchored at the injection orifice. The flame stabilizes closer to the injection plate for smaller reactant flow rates or higher equivalence ratios. This originates a higher flame temperature due mainly to the increased thermal resistance from the flame region to the external ambient. The higher flame temperature is helpful for the combustion of very diluted mixtures (or low heat content fuels) thus expanding the lean flammability limit, but it may also result in higher production of NO_x .

In the past years, emission regulations for industries have become ever more stringent. The need to a more rational use of available energy has also lead to replacement of existing electrical infrared by natural gas heating. The

application of porous radiating burners in the interior of furnaces requires the operation under a usually hot environment and very few works have focused the operation of PRB in hot environments.

Here, an experimental study of combustion characteristics of a PRB operating in a confined hot environment, such as pollutant emissions and flame stability limits, is performed. In the following, the experimental apparatus and uncertainties are described. Then, the measurements are presented and discussed. Finally, conclusions and recommendations about the burner operation are summarized.

2. EXPERIMENTAL SET UP

The experimental set up to test the PRB is composed of a burner section, an air and fuel supply systems, a laboratory-scale furnace, monitored by temperature and chemical species measurement systems. The air supply system is composed of an air compressor and tank, a pressure control valve, a shut-off valve, a flow control valve and a calibrated rotameter, with measurement range between 0 and 92 liters per minute (lpm). The fuel supply system is composed of a pressurized gaseous fuel bottle, a pressure control valve, a shut-off valve, a flow control valve and an electronic flow meter with the measurement range between 0 and 30 lpm. The gaseous fuel used is 99.8% pure methane. The methane and air are mixed in a mixing pipe with length of 1000 mm and diameter of 40 mm. At the end of the mixing pipe, a bed of glass beads is used as a laminarization section.

The laboratory-scale furnace used in this study simulates industrial hot equipment. It is built from a vertical stainless steel cylinder with a diameter of 200 mm and a length of 1500 mm. The walls are heated by electrical resistances. The wall temperatures are controlled by a temperature controller (2132 – *Eurotherm Controls*) that includes thermocouples of type K. The PRB is placed on the bottom of the furnace.

The PRB is made with layers of ceramic foams composed of alumina (Al_2O_3) and zirconia (ZrO_2), each of which with a diameter of 70 mm and a thickness of 20 mm (manufactured by *Foseco Ltda.*). The first region, called pre-heating region (PR), is made with a 40 porous per inch (ppi) ceramic foam and the second region, called stable-burning region (SBR), is made with a 10 ppi ceramic foam. All foams have 80% of volumetric porosity. An injection plate with a single central orifice is placed upstream from the ceramic foams, as shown in Fig. 1.

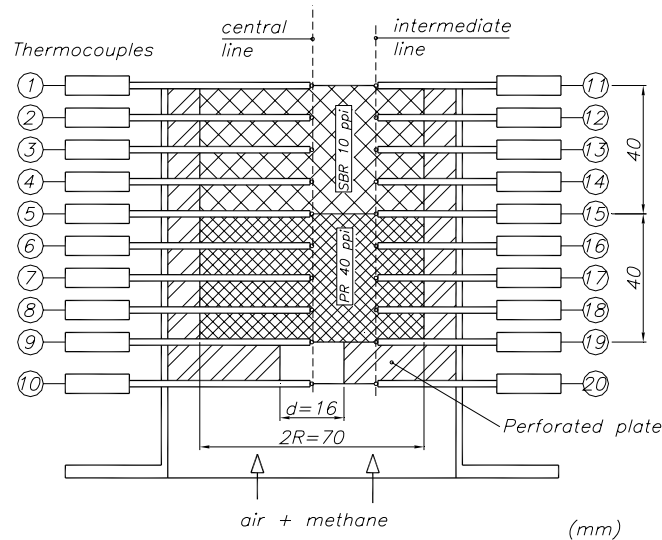


Figure 1. Schematic drawing of the radiant porous burner (PRB).

Type R (platinum and platinum + 13% rhodium, from *Omega Engineering*) thermocouples placed inside alumina double-holed tubes are used to measure the temperature within the porous matrix. The thermocouple measurements are recorded by a data acquisition system (34970A - *Agilent*) interfaced with a computer. The chemical species measurement system is composed of the alumina pipe probe, a condenser, a dryer, a particulate filter, a pump, a rotameter and the gas analyzers. To avoid the condensation of the water vapor and the possible dilution of the NO_2 in the condensed water, the collector pipe line is heated by an electrical resistance. The gas analyzers included a magnetic pressure analyzer for O_2 measurements, nondispersive infrared gas analyzers for CO_2 and CO measurements (both CMA-331A - *Horiba*), a flame ionization detector for hydrocarbons measurements (FID E 2020 - *Amluk*) and a chemiluminescent analyzer for NO_x measurements (CLA-510 SS - *Horiba*). The experiments were run either in the confined environment or in open ambient. In the open environment tests, the combustion products samples were collected in the central line on the burner surface (Fig. 1). In the confined tests, due to limitation of the experimental apparatus, the samples were collected on the upper opening of the furnace (chimney), where the composition of the combustion products is homogeneous. Note that these gas sampling processes result in different measurements, since, in the confined ambient, the gases flow along the oven prior collection, while in the open ambient the gases were collected

right at the point where they left the burner. From the measurements of the concentration of the major species in the combustion products, the CO and NO_x emission index (EI) were calculated from

$$EI_i = \left(\frac{X_i}{X_{CO} + X_{CO_2}} \right) \left(\frac{xMW_i}{MW_f} \right), \quad (1)$$

where X_i represents the molar fraction of species i , x is the number of carbon atoms in the chemical formula for the primary fuel and MW_i and MW_f are the molar mass of species i and fuel, respectively. The unburnt hydrocarbon concentrations were smaller than 2 ppm and were not included in the emission index equation.

The experimental procedure to find the stability limits, based on the procedure of Hsu et al. (1993), is reported in detail in Catapan (2007). First, the fuel equivalence ratio and a volumetric flow rate that allows for stable flame propagation within the porous burner was set. The equivalence ratio was then slowly adjusted to the test value and the volumetric flow rate was increased until the upper limit of flame stability (the blow-out limit) was reached. Then, the burner was reinitialized and the volumetric flow rate was decreased until the lower limit of flame stability (the flashback limit) was reached. The blow-out and flashback limits were detected with the aid of the temperature measurements. The flash back is defined as the point when the temperature of the distribution plate reaches a high limiting value, while the blow out limit is defined as the point when the surface temperature reaches the higher value among all the temperatures recorded within the porous medium. The larger fuel equivalence ratio tested was limited by the degradation temperature of the porous matrix and the injection plate, which are 1600 °C and 1200 °C, respectively. Here, the fuel equivalence ratio follows the usual definition, *i.e.*,

$$\Phi = \frac{\left(\frac{\dot{m}_F}{\dot{m}_a} \right)_a}{\left(\frac{\dot{m}_F}{\dot{m}_a} \right)_s} \quad (2)$$

where \dot{m}_F is the fuel mass flow rate, \dot{m}_a is the air mass flow rate, the subscript s stands for stoichiometric conditions and the subscript a stands for actual conditions.

The flame speed is defined as the ratio between the unburnt reactants volumetric flow rate and the burner area.

The experimental uncertainties of the measurements were determined from an error propagation analysis and are presented in Tab. 1.

Table 1. Experimental uncertainties.

Variable, unit	T, °C	Φ	S_L , cm/s	EINO _x , g/kg	EICO, g/kg
IM, %	± 5 %	± 10 % (for $S_L > 10$ cm/s)	± 5 %	± 30 %	± 60 %

3. RESULTS AND DISCUSSIONS

3.1. Stability limits

The stability experiments were performed in open and hot confined environment at equivalence ratios ranging from 0.40 to 0.65. The maximum total power was 4.0 kW at $\Phi = 0.65$ and $S_L = 50$ cm/s and the minimum total power was 0.6 kW at $\Phi = 0.40$ and $S_L = 12$ cm/s.

Figure 2 shows the stability limits of PRB in open environment. It can be identified three different regions, named the blow-out region, the stable-flame region and the region of thermal damage of the injection plate. The upper line is the blow-out limit. In general, the blow-out occurs in the central region of the surface burner as a consequence of the conical shape of the flame front (Catapan et al., 2006). Flashback was not observed for the equivalence ratios studied. The lower limit corresponds to a high temperature in the injection plate, close to its degradation temperature. This limit is reached when the volumetric flow rate decreases and the flame front moves closer to the injection plate (Catapan et al., 2006). Along the lower line, the porous matrix temperature remained below its maximum allowed temperature. The porous matrix degradation temperature was reached for the higher equivalence ratio (0.65) when the flame velocity exceeds 40 cm/s, prohibiting a further increase in equivalence ratio.

Figure 3 shows the stability limit for the PRB used in the present work and the PRB used in Pereira (2002). The difference in the two works is the flame shape stabilized within the porous burner. While in Pereira (2002) the flame was plane and stabilized at the porous layers interface (there was no injection hole), in the present study the flame is conical and stabilized at the rim of the injection hole. Higher upper and lower stability limits are achieved for $\Phi < 0.55$

for the conical flame. This is probably related to the larger surface area exhibited by the conical flame when compared to the plane flame, resulting in higher total power (higher flame speed) for the same equivalence ratio. In addition, the injection plate acts as a thermal insulation to the upstream current, generating a higher flame temperature and, consequently, a higher local flame speed. Therefore, the blow-out occurs in a higher volumetric flow rate than in a PRB without an injection plate.

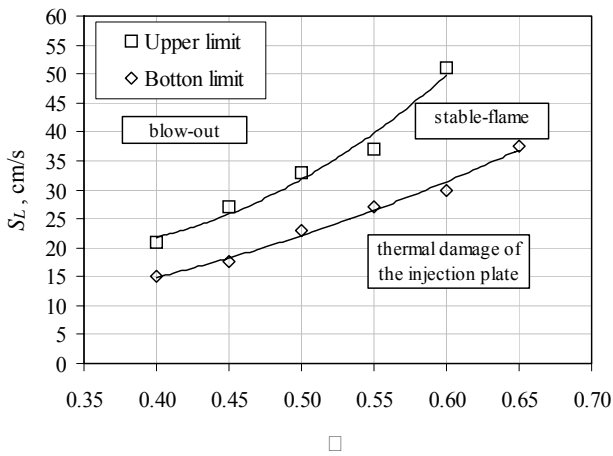


Figure 2. Flame stability limits for the PRB in open environment operation.

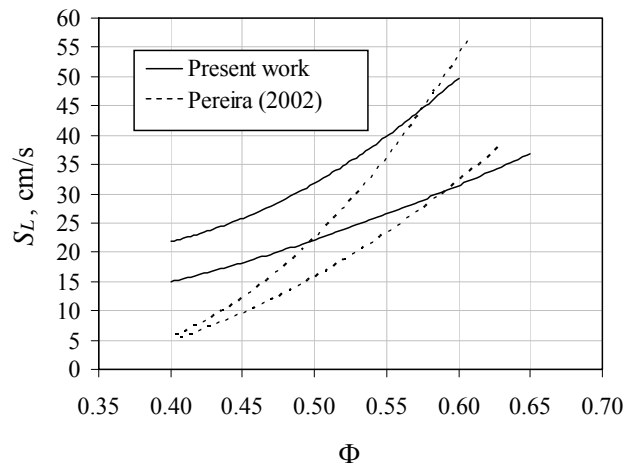


Figure 3. Stability limits for the PRB used in the present work (continuous line) and the PRB used in Pereira (2002) (dashed line).

Figure 4 shows the stability limits of the PRB in the hot environment operation, with a furnace temperature of 950 °C. The PRB operation was strongly limited by the porous matrix temperature, allowing only equivalence ratios smaller than 0.60. Even so, the range of flame stability is almost the same for both confined and open environment operation on each equivalence ratio. Flashback was not observed in any equivalence ratio. Differently to open environment operation, the lower stability limit occurs due to porous matrix temperature. This difference can be related to the smaller heat loss from porous matrix to surroundings in the hot environment operation, resulting in a higher temperature within the porous medium.

It is interesting to note that for higher furnace temperature and for higher volumetric flow rates, the flame experiences a transition from the conical to a plane shape and stabilizes at the end of the stable-burning region, very close to the burner surface. This transition of flame shape regime is showed in Fig. 4, separating the upper region, where plane flames are observed, from the lower region where conical flames are observed. Even though the flame shape changes for higher surface temperature, the upper stability limits remain almost the same when compared to the operation in an open environment. The behavior observed for lower furnace wall temperatures (500 °C) is qualitatively equivalent to the open flame.

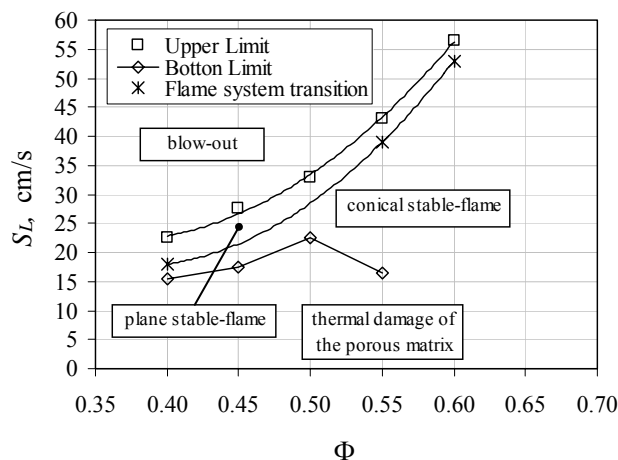


Figure 4. Stability limits of the PRB in the hot environment operation, for wall temperature of the furnace of 950°C.

3.2. Pollutant emissions

Under open environment operation, the PRB presented EINO_x values between 0.10 g/kg and 0.50 g/kg and EICO values between 0.05 g/kg and 3.72 g/kg. These results are consistent with the results presented by Mital et al. (1997).

Under hot environment operation, the $EINO_x$ values varied between 0.05 g/kg and 0.35 g/kg and the EICO values varied between 0.04 g/kg and 0.35 g/kg. No emissions measurements were found in the literature for confined operation.

3.2.1. Effect of flame speed

Figure 5 presents the $EINO_x$ as a function of the flame speed and equivalence ratio for open environment operation. In general, the $EINO_x$ increase when the flame speed decreases. This can be attributed to two reasons that influence the NO formation via the thermal mechanism. First, there is the increase of the residence time of the combustion products in the hot region and, second, the increase of the flame temperature within the reaction zone. This second effect can be explained as follows. Fig. 6 presents the flame temperature (T_{fl}), here defined as the maximum temperature within the porous matrix, for each experimental condition, as a function of the flame speed and equivalence ratio. For all equivalence ratio studied, the flame temperature increases when the flame speed is decreased. In the PRB with an injection plate, the flame front moves closer to the injection plate when the flame speed decreases (Catapan et al., 2006). Thus, the length of porous matrix downstream from the flame front is larger, decreasing the heat loss from the plate to the surroundings. Therefore, the flame temperature is higher when the flame stabilizes closer to the injection plate as a result of the increased thermal resistance to axial heat loss to the external environment. Consequently, both the flame temperature and $EINO_x$ increase, even when the total power decreases.

These results are opposed to results presents in the literature (Hsu et al., 1993; Khanna et al., 1994 and Mital et al., 1997) where the NO_x emission decreases when the flame speed decreases. In those studies, however, the flame stabilizes at the interface between the ceramic foam layers and therefore the flame position does not change appreciably with the flame speed. Consequently, the flame temperature and the NO_x emission depend only on total power, which decreases when the flame speed decreases.

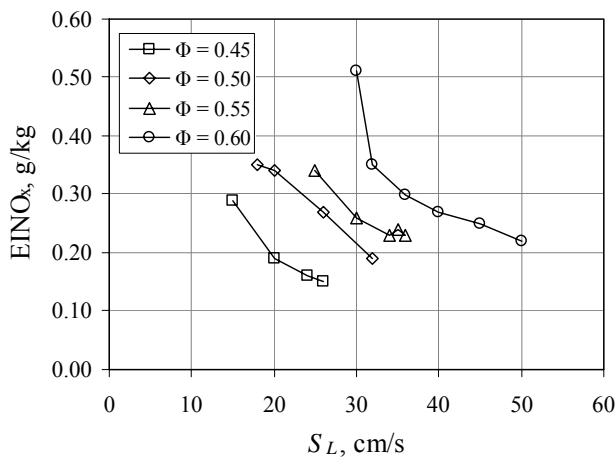


Figure 5. $EINO_x$ as a function of the flame speed and equivalence ratio for open environment operation.

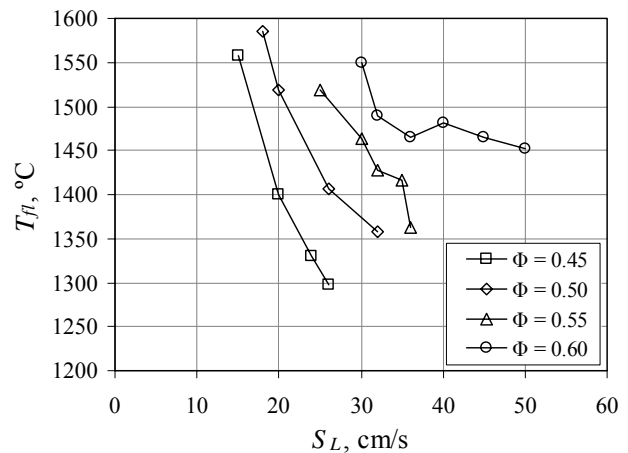


Figure 6. Flame temperature (T_{fl}) as a function of the flame speed and equivalence ratio.

Figure 7 presents the EICO as a function of the flame speed and equivalence ratio for open environment operation. It can be noted that the EICO increases with the flame speed. Similarly to NO_x emissions, the CO emissions are strongly influenced by the residence time and flame temperature. But here, for higher flame speeds, the lower residence time and lower flame temperature increase de EICO. This tendency for the increase in CO emissions with the flame speed was discussed in the literature (Hsu et al., 1993 and Khanna et al., 1994).

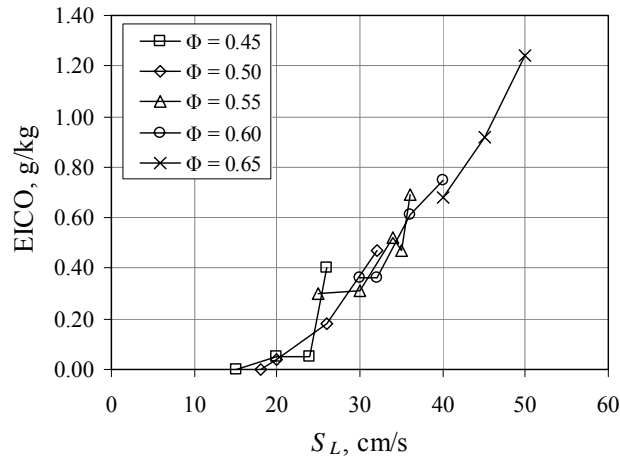


Figure 7. EICO as a function of the flame speed and equivalence ratio, for open environment operation.

3.2.2. Effect of equivalence ratio

The effect of equivalence ratio on the $EINO_x$ can be explained from Figs. 5 and 6. For the same flame speed, the higher equivalence ratios result in higher $EINO_x$. It can be observed that the flame temperature increases with the equivalence ratio. Similarly to a decrease in flame speed, the flame front moves closer to the injection plate when the equivalence ratio is increased, increasing the flame temperature and also the residence time. In addition, the formation of NO via the prompt mechanism is favored in higher equivalence ratios. These results are consistent with those presented by Mital et al. (1997).

Table 2 presents the minimum and the maximum EICO for each equivalence ratio. The stable flame ranges are also presented. It can be noted that the EICO range increases with the equivalence ratio. The CO oxidation is slower at higher equivalence ratio due to smaller excess air. However, the larger range for stable flame occurs for higher equivalence ratio. Therefore, the higher CO emissions are a result of the lower residence times, lower flame temperatures and lower air excess levels.

Table 2. Stable flame range, minimum and maximum EICO for each equivalence ratio.

Φ	Stable S_L range, cm/s	$EICO_{min}$, g/kg	$EICO_{max}$, g/kg
0.45	15 a 26	0.00	0.40
0.50	18 a 32	0.00	0.47
0.55	25 a 36	0.30	0.59
0.60	30 a 50	0.36	1.24

3.2.3. Effect of environment temperature

Figure 8 presents the $EINO_x$ as function of the furnace temperature (T_f) for a flame with $\Phi = 0.55$ and $S_L = 30$ cm/s. These measurements were taken for successive increments of the furnace wall temperature. Each measurement represents a steady state condition. It can be observed that the $EINO_x$ increases from 0.12 g/kg to 0.29 g/kg for $T_f = 250$ °C to $T_f = 950$ °C, respectively. In these experimental conditions, the flame temperature varied from 1440 °C to 1500 °C. In this temperature range, the equilibrium molar fraction of NO and NO₂ is strongly dependent on flame temperature. For a mixture of combustion products CO₂, H₂O, O₂, N₂, CH₄, NO, NO₂ and H₂, resulting from the combustion of methane in air, the equilibrium concentration of NO_x for $T_{fl} = 1500$ °C is 25% higher than that for $T_{fl} = 1440$ °C (Reynolds, 1986). Therefore, although the measured values are below the equilibrium values, the measured increase is in the direction of chemical equilibrium. This indicates that the flame temperature and, consequently, the NO_x emission must be controlled in a hot environment operation of a PRB.

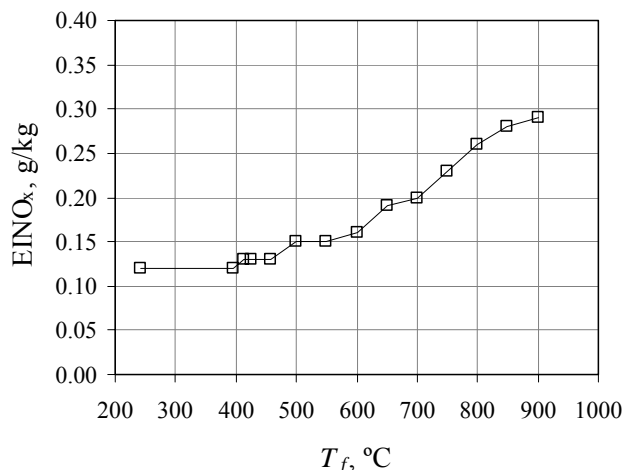


Figure 8. EINO_x as function of the furnace temperature for a flame with $\Phi = 0.55$ and $S_L = 30$ cm/s.

Figure 9 presents the EICO as function of the furnace temperature for a flame with $\Phi = 0.55$ and $S_L = 30$ cm/s. The EICO decreases when the furnace temperature is increased. Note that the measurement of combustion products composition is made in the furnace outlet. Therefore, the residence time of the combustion products is higher than in open environment. In addition, the heat loss from combustion products to the furnace wall decreases when the furnace temperature is increased, keeping the gas at higher temperature while it flows along the furnace. Because of these reasons, there is additional CO oxidation inside the furnace.

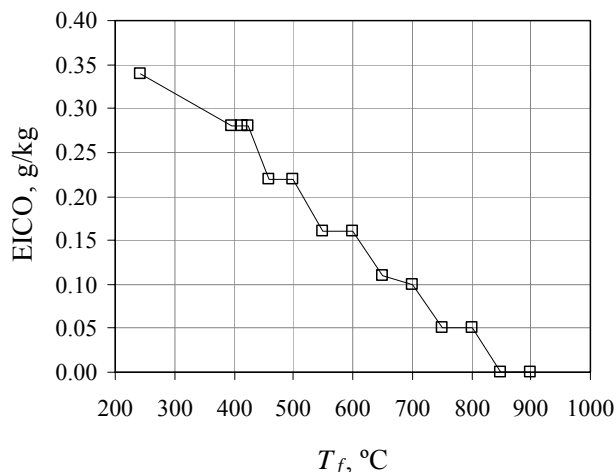


Figure 9. EICO as a function of the furnace temperature for a flame with $\Phi = 0.55$ and $S_L = 30$ cm/s.

For the same furnace wall temperature, both the flame speed and the equivalence ratio effects on EINO_x were almost the same than the observed in open environment operation. However, in contrast with open environment operation, the EICO is smaller at higher equivalence ratio, when the furnace wall temperature is kept constant. This can be related to the higher flow temperature that promotes CO oxidation inside of the furnace.

4. CONCLUSIONS

A detailed experimental study of the combustion characteristics, such as the stability limits and the pollutant emissions, of a porous radiant burner (PRB), burning premixed methane and air, in a confined hot environment is presented. The PRB employs a single hole injection plate as the flame stabilizing mechanism. A laboratory-scale furnace with controlled wall temperatures is used. The local temperature and major species concentration are measured on the PRB and on the furnace, respectively. For comparisons purposes, tests in an open environment are also presented. The main results of this study can be summarized as follows:

1. The range of flame stability is almost the same for both confined and open environment operation. The confined environment operation is strongly limited by the porous matrix degradation temperature, allowing only the combustion of mixtures with equivalence ratio smaller than 0.60.

2. Flashback was not observed for any of the experimental conditions. Under open environment operation, the lower stability limit occurs when the injection plate reaches its degradation temperature. Conversely, under confined environment operation, the lower stability limit occurs when the porous matrix reaches its degradation temperature. This difference can be related to the smaller heat loss from the porous matrix to surroundings in the hot environment operation.
3. For higher reactant flow rates and higher furnace wall temperature, the flame experiences a transition from the conical to a plane shape and stabilizes at the end of the stable-burning region, very close to the burner radiant surface. Even though the flame shape changes for higher surface temperature, the upper stability limits remain almost the same when compared to the operation in an open environment.
4. For the same experimental condition, the $EINO_x$ increases with the furnace wall temperature. This occurs due to the increase in the flame temperature. Conversely, the EICO decrease with the furnace wall temperature. This is related to higher flame temperature and CO oxidation inside of the furnace.
5. For the same furnace wall temperature, both the flame speed and the equivalence ratio effects on $EINO_x$ were almost the same than the observed under open environment operation. However, in contrast with operation under open environment, the EICO is smaller in higher equivalence ratio, when the furnace wall temperature is kept constant. This can be related to the higher flow temperature that promotes CO oxidation inside of the furnace.

5. ACKNOWLEDGMENTS

This work was developed under a CAPES-GRICES cooperation program between the Universidade Federal de Santa Catarina and the Instituto Superior Técnico de Lisboa. The experiments were performed in the Laboratório de Combustão at the Instituto Superior Técnico. The authors acknowledge the assistance of Mr. Manuel Pratas from IST. The authors also acknowledge the financial support of the program ANP PRH-09/MECPETRO in the form of a graduate scholarship.

6. REFERENCES

- Barra, A. J.; Diepvens, G.; Ellzey, J. L.; Henneke, M. R. Numerical study of the effects of material properties on flame stabilization in a porous burner. *Combustion and Flame*, v. 134, pp. 369-379, 2003.
- Barra, A. J.; Ellzey, J. L. Heat recirculation and heat transfer in porous burners. *Combustion and Flame*, v. 137, pp. 230-241, 2004.
- Brenner, G.; Pickenacker, K.; Pickenacker, O.; Trimis, D.; Wawrzinek, K.; Weber, T. Numerical and experimental investigation of matrix-stabilized methane/air combustion in porous inert media, *Combustion and Flame*, v. 123, pp. 201–213, 2000.
- Catapan, R. C.; Pereira, F. M.; Oliveira, A. A. M. Development of a radiant porous burner with a combined thermal and fluiddynamic mechanism of flame stabilization. In: INTERNATIONAL CONGRESS OF MECHANICAL ENGINEERING, 18, Ouro Preto, Brasil, 2005.
- Catapan, R. C.; Pereira, F. M.; Oliveira, A. A. M. Experimental study of a combined thermal and fluiddynamic mechanism of flame stabilization in a radiant porous burner. In: BRAZILIAN CONGRESS OF THERMAL SCIENCES AND ENGINEERING – ENCIT, 11, Curitiba, Brasil, 2006.
- Catapan, R. C., Study of the combined thermal and fluid-dynamic stabilization mechanism in a porous radiant burner and its operation in a high temperature environment, Mechanical Engineering Graduate Program, UFSC, 2007 (in Portuguese).
- Ellzey, J. L. and Goel, R. Emissions of CO and NO from a two stage porous media burner. *Combustion Science and Technology*, v. 107, pp. 81-91, 1995.
- Howell, J. R.; Hall, M. J.; Ellzey, J. L. Combustion of hydrocarbon fuels within porous inert media. *Progress in Energy and Combustion Science*, v. 22, pp. 121-145, 1996.
- Hsu, P. F. Experimental study of the premixed combustion within the nonhomogeneous porous ceramic media. In: NATIONAL HEAT TRANSFER CONFERENCE, 6, ASME, 1996.
- Hsu, P. F., Evans, W. D., Howell, J. R. Experimental and numerical study of premixed combustion within nonhomogeneous porous ceramics. *Combustion Science and Technology*, v. 90, pp. 149-172, 1993.
- Hsu, P. F.; Matthews, R. D. The necessity of using detailed kinetics in models for premixed combustion within porous media. *Combustion and Flame*, v. 93, pp. 457-466, 1993.
- Khanna, R.; Goel, R.; Ellzey, J. L. Measurements of emissions and radiation for methane combustion within a porous medium burner. *Combustion Science and Technology*, v. 99, pp. 133-142, 1994.
- Kotani, Y.; Takeno, T. An experimental study on stability and combustion characteristics of an excess enthalpy flame. *Proceedings of the Combustion Institute*, 19, pp. 1503-1509, 1982.
- Kotani, Y.; Behbahani, H. F.; Takeno, T.. An excess enthalpy flame combustor for extended flow ranges. *Proceedings of the Combustion Institute*, 20, pp. 2025-2033, 1984.

- Mishra, S.C.; Steven, M.; Nemoda, S.; Talukdar, P.; Trimis, D.; Durst, F. Heat transfer analysis of a two-dimensional rectangular porous radiant burner. *International Communications in Heat and Mass Transfer*, v. 33, pp. 467–474, 2006.
- Mital, R.; Gore, J. P.; Viskanta, R. A study of the structure of submerged reaction zone in porous ceramic radiant burners. *Combustion and flame*, v. 111, pp. 175-184, 1997.
- Pereira, F. M. Measurement of the thermal characteristics and study of the flame stabilization mechanism in porous radiant burners, Mechanical Engineering Graduate Program, UFSC, 2007 (in Portuguese).
- Reynolds, W. C. The element potential method for chemical equilibrium analysis: Implementation in the interactive program STANJAN 3. Stanford University, 1986.
- Sathe, S. B.; Kulkarni, M. R.; Peck, R. E.; Tong, T. W. An experimental and theoretical study of porous radiant burner performance. *Proceedings of the Combustion Institute*, 23, pp. 1011-1018, 1990a.
- Sathe, S. B.; Peck, R. E.; Tong, T. W. A numerical analysis of heat transfer and combustion in porous radiant burners. *International Journal of Heat and Mass Transfer*, v. 33, pp.1331-1338, 1990b.
- Takeo, T., Sato, K. An excess enthalpy flame theory. *Combustion Science and Technology*, v. 20, pp. 73-84, 1979.
- Talukdar, P.; Mishra, S. C.; Trimis, D.; Durst, F. Heat transfer characteristics of a porous radiant burner under the influence of a 2-D radiation field. *Journal of Quantitative Spectroscopy and Radiative Transfer*, v. 84, pp. 527–537, 2004.
- Trimis, D.; Durst, F. Combustion in a porous medium – advances and applications. *Combustion Science and Technology*, v. 121, pp. 153-168, 1996.
- Yoshizawa, Y.; Sasaki, K.; Echigo, R. Analitical study of the structure of radiation controlled flame. *International Journal of Heat and Mass Transfer*, v. 31, pp. 311-319, 1988.

7. RESPONSIBILITY NOTICE

The authors are the only responsible for the printed material included in this paper.